Novel Dopamine-Modified Cellulose Acetate Ultrafiltration Membranes with Improved Separation and Antifouling Performances

Xi Ma
Northeast Forestry University
Hanxiang Guo
Northeast Forestry University
Zhaofeng Wang
Northeast Forestry University
Nan Sun
Northeast Forestry University
Pengfei Huo
Northeast Forestry University
Jiyou Gu
Northeast Forestry University
Yang Liu (liuyang@nefu.edu.cn)
Northeast Forestry University

Research Article

Keywords: Ultrafiltration membrane, Antifouling property, Dopamine, Cellulose acetate

Posted Date: September 28th, 2021

DOI: https://doi.org/10.21203/rs.3.rs-914543/v1

Version of Record: A version of this preprint was published at Journal of Materials Science on March 8th, 2022. See the published version at https://doi.org/10.1007/s10853-022-07024-y.

Novel dopamine-modified cellulose acetate ultrafiltration membranes with improved separation and antifouling performances

Xi Ma · Hanxiang Guo · Zhaofeng Wang · Nan Sun · Pengfei Huo · Jiyou Gu · Yang Liu

X. Ma · H. Guo · Z. Wang · N. Sun · P. Huo · J. Gu · Y. Liu(✉)

Key Laboratory of Bio-based Materials Science & Technology, Ministry of Education, College of Material Science and Engineering, Northeast Forestry University, Harbin 150040, PR China

e-mail: liuyang@nefu.edu.cn

X. Ma and H. Guo contributed equally.

Abstract Cellulose derivatives are the earliest and most widely used membrane materials due to its many excellent characteristics, especially chemical activity and biodegradability. However, the hydrophobic properties of cellulose acetate (CA) limited its development to some extent. To improve the inherent hydrophobic and antifouling properties of the CA membrane, CA was successfully modified with dopamine (CA-2,3-DA) through selective oxidation and Schiff base reactions in this work, which was confirmed by ^{1}H NMR and FTIR measurements. And then, the CA-2,3-DA membrane with high water permeability and the excellent antifouling property was prepared by the phase inversion method. Compared with the primordial CA membrane, the CA-2,3-DA membrane maintained a higher rejection rate for BSA (92.5%) while greatly increasing the pure water flux (167.3 L/m^{2}h), which could be overcome the trade-off relationship between selectivity and permeability of the traditional CA membrane to a certain extent. According to the three-cycles dynamic ultrafiltration and static protein adsorption experiments, the CA-2,3-DA membrane showed good long-term performance stability and superior antifouling performance, which was supported by the experiment results including filtration resistance, flux decline ratio and flux recovery ratio. It is expected that this approach can greatly expand the high-value utilization of modified natural organic polysaccharides in separation engineering.

Graphical abstract

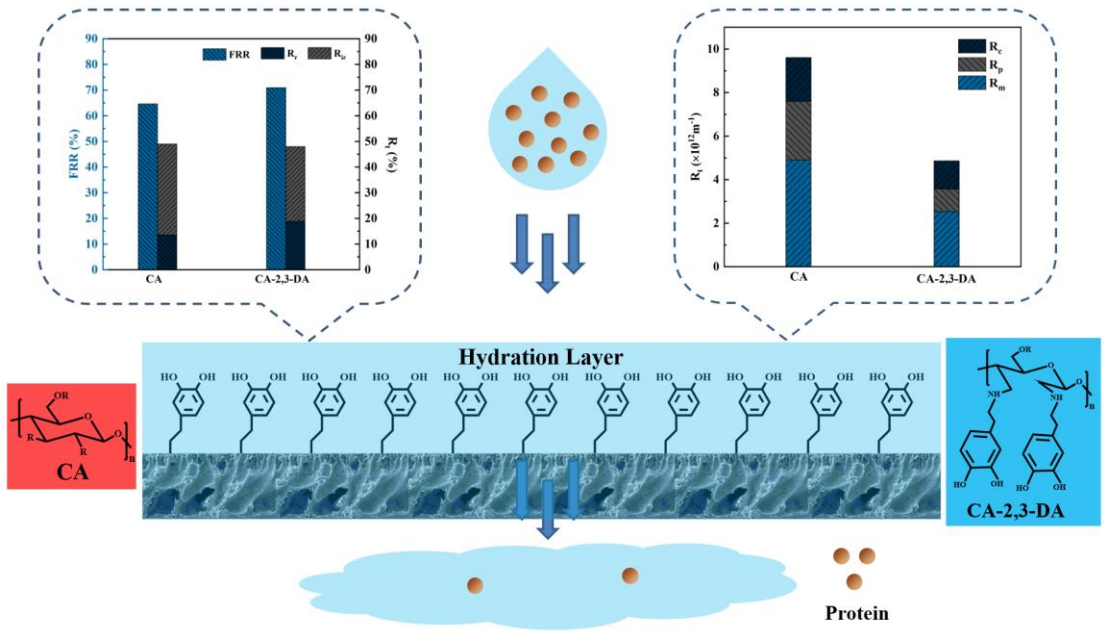

Keywords Ultrafiltration membrane • Antifouling property • Dopamine • Cellulose acetate

Introduction

Membrane separation technology is composed of membrane distillation (MD), reverse osmosis (RO), nanofiltration (NF), ultrafiltration (UF), and microfiltration (MF), which has the characteristics of high separation efficiency, low energy consumption, and no pollution to the environment (Mokhena et al. 2017). In the context of global water resource shortage and deteriorating natural conditions, membrane separation technology as an efficient means of water treatment has attracted widespread attention. Among them, the molecular weight cutoff of ultrafiltration membrane can be controlled in 10^3~10^6 Da, and the pore size can be adjusted in the range of 10~100 nm (Karami et al. 2020), which can effectively intercept proteins, viruses, dyes and other macromolecules, etc. In the current global outbreak of COVID-19, the unique advantages of ultrafiltration membranes are further highlighted. Due to its many advantages, ultrafiltration technology has been diffusely employed in effluent treatment, oil-water separation, biomedicine and the food industry (Park et al. 2017). The membrane material is the main factor to determine the membrane performance. Currently, polymer materials including cellulose and its

derivatives (Oprea and Voicu 2020), polysulfone (Liu and Kim 2011), polyolefins (Wang et al. 2020) and fluorinated materials (Yu et al. 2021) are most widely used in the field of membrane separation technology. However, due to the inherent hydrophobic properties of these membrane materials, they are easily contaminated during ultrafiltration process (Li et al. 2015).

Membrane fouling augments the filtration resistance, and even clogs the membrane hole, thus reducing the filtration efficiency, shortening the service life, greatly increasing the operating cost of membrane modules (Wang and Liu 2021; Zhang et al. 2012). To some extent, it hinders the application and development of membrane technology. To improve antifouling performance, various methods such as additive blending (Zhu et al. 2015), surface coating (Yang et al. 2012) and chemical modification (Keating et al. 2016; Liu et al. 2017) have been studied. In addition to the above research strategies, dopamine as an exciting candidate material in the field of separation technology is also increasingly concerned. Dopamine is a small molecule containing both alkylamine and catechol groups(Cheng et al. 2020), which is often used as an additive to blend with polymer matrix to improve the hydrophilicity of various membranes. Tian et al. prepared polydopamine modified MoS_2 (MoS_2@PDA) blend polyethersulfone ultrafiltration membrane. The membrane has excellent water permeability and selectivity, especially the rejection ratio of Janus Green B is as high as 99.88% (Tian et al. 2021). Mu et al. modified hydroxyapatite nanotubes via polydopamine and polyethylenimine co-deposition (HANTs@PDA/PEI), and added them to carboxylated polysulfone matrix to prepare ultrafiltration membrane. The results showed that compared with the unfilled membrane, the pure water flux of the hybrid membrane increased by 3.2 times, and the flux recovery ratio for BSA solutions reached 90.8% while achieving high flux (Mu et al. 2020). Parashuram et al. fabricated hybrid ultrafiltration membranes using different sulfonated functionalized polydopamine (SPDA) loading levels with polyethersulfone as polymer matrix, which significantly improved the antifouling performance of the membrane (Kallem et al. 2021). In some ways, although additive blending modification has significant advantages, there is generally no chemical bond between additive and polymer matrix, which makes modifiers easy to migrate, deteriorating the membrane selectivity and long-term stability.

Dopamine shows great potential in surface modification of water purification membrane because it provides a facile route to hydrophilization of the membrane surfaces to improve its antifouling performance. Choi et al. fabricated multifunctional coating materials with biofouling

and oil-fouling-resistant and bactericidal properties using monomers containing mussel-inspired dopamine and plant-based cardanol groups (Choi et al. 2014). Chen et al. used polydopamine to graft activated GO nanosheets onto ultrafiltration membranes to enhance their antifouling properties (Chen et al. 2020). Li et al. reported a method for the modification of mussel-inspired polyvinylidene fluoride (PVDF) membranes by inkjet printing with dopamine and then under UV light irradiation. The optimized membrane exhibited superior oil/water separation efficiency and antifouling performances, and the oil rejection ratio is more than 99% (Li et al. 2021). The above methods of surface modification have a significant effect on improving membrane performance in a short time (Xie et al. 2021). However, due to the self-polymerization and migration of dopamine in the process of modification and use, it agglomerates on the surface of the membrane and thus leads to the stoppage of membrane pore channels. Meanwhile, the surface modification method has poor repeatability, and it is difficult to achieve large-scale industrial production. Therefore, there is an urgent need for a kind of membrane material that not only has long-term stable separation and antifouling performances but also can realize continuous large-scale production.

Cellulose is a natural polymer with the largest reserves in nature. The hydroxyl group in the molecule has strong reactivity and is easy to undergo chemical modification such as esterification (Rafieian et al. 2020) and amidation (Zhou et al. 2021) to prepare cellulose derivative for different applications. Among them, cellulose acetate (CA) obtained by acetylation part of a hydroxyl group on cellulose is a promising membrane material with good pore-forming performance, high selectivity and large water flux, etc (Silva et al. 2021). Also, because cellulose acetate is the product of incomplete esterification and contains a large number of active sites, it has broad room for further modification. Given the above-mentioned advantages of cellulose acetate and dopamine, this paper reported a novel material that CA was successfully modified with dopamine (CA-2,3-DA) through selective oxidation and Schiff base reactions. Then, CA-2,3-DA and CA were used as raw materials to prepare ultrafiltration membranes, and the CA membrane was the control group. The experimental results showed that the introduction of dopamine can significantly enhance comprehensive separation and antifouling performances of the membrane. CA-2,3-DA is expected to be widely adopted in various industrial purification and separation fields, thereby realizing the deep and high value-added utilization of cellulose derivative materials.

Experimental Part

Materials

Cellulose acetate (CA, 39 wt% acetyl), dopamine hydrochloride, polyvinylpyrrolidone (PVP 30K) and sodium periodate were all supplied by Aladdin Reagent, China. Phosphate buffer solution (PBS, pH=7.4, 0.1 mol/L) and bovine serum albumin (BSA)were purchased by Dingguo BioTechnology Co. Ltd. (China). Calcium chloride, sodium borohydride and N,N-dimethyl acetamide (DMAc), were used as received from Beijing Chemical Reagent, China.

Preparation of dopamine-modified cellulose acetate (CA-2,3-DA)

The preparation of dopamine-modified cellulose acetate involves two steps: selective oxidation and Schiff base reactions. The specific process is shown in scheme 1.

Dialdehyde acetate cellulose (DAC): Under nitrogen atmosphere and light-proof conditions, 15 g cellulose acetate was suspended in 300 mL deionized water. Then, 15 g of sodium periodate and 22.5 g of calcium chloride were added to the system and stirred at 45 °C . After 6 h, 75 mL of glycol was added to react with excess sodium periodate in the system. After the reaction was complete (about 0.5 h), the sublayer precipitation was separated and cleaned repeatedly with deionized water. Finally, vacuum drying was performed.

CA-2,3-DA: First, 3.0 g of DAC was dissolved in 30 mL DMAc. Then, 1.0 g of dopamine hydrochloride was slowly added to the solution, which reacted for 12 h at 50 °C. Then, 0.45 g of sodium borohydride was added to the system to continue the reaction for 3 hours. After the reaction, the products were washed thoroughly in distilled water and ethanol respectively and dried at 60 °C for 12h under vacuum to obtain the final CA-2,3-DA.

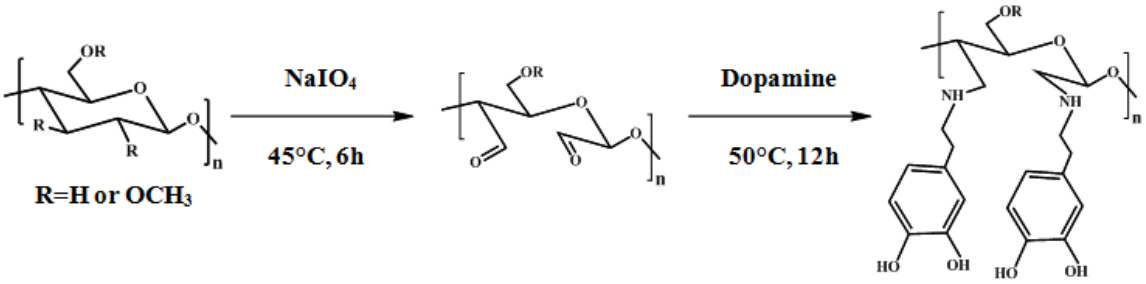

Scheme 1. Preparation route of CA-2,3-DA.

Preparation of ultrafiltration membrane

The polymer (CA or CA-2,3-DA, 15 wt%) and pore-forming agent PVP (3 wt%) were dissolved in DMAc (82 wt%) to prepare the casting solution. When there were no bubbles in the system, used a casting knife having a thickness of approximately 200 μm to evenly spread the casting solution on a clean glass plate. To evaporate the solvent, put it in the air for a period of time, and transferred it into deionized water to allow the solvent, pore-forming agent and non-solvent to diffuse in both directions. Two prepared membranes were rinsed several times by deionized water to wash away the residual solvent and water-soluble pore-former, and then preserved in fresh ultrapure water for further characterizations.

Characterization

Bruker Vertex 80V FTIR and Bruker 510 ^{1}H NMR spectrometer were applied to explore the chemical structure changes of CA before and after modification. The thermal stability of CA and CA-2,3-DA were ananlyzed by TGA (Perkin-Elmer Pyris 1) in the nitrogen atmosphere, and the heating rate was 10 °C/min. SEM (JEOL JSM-7500F) was used to characterize the surface and cross-section morphology of the ultrafiltration membrane. The sample section was obtained by the liquid nitrogen freezing fracture method, and gold spraying was performance before imaging.

To obtain pure water contact angle (WCA) data, samples are measured by a contact angle goniometer (KRUSS GMBH, Hamburg 100). Each sample was tested more than five times. Based on the WCA data, the surface free energy can be calculated by the following formula:

$$cos\theta = -1 + 2\sqrt{\frac{\gamma_s}{\gamma_l}}e^{-\beta(\gamma_s-\gamma_l)^2} \quad (1)$$

Where β is a constant of 0.0001247, θ stands for contact Angle. γ_l and γ_s are the surface free energy of the feed and membrane, respectively.

By weighing the mass of the membrane in both dry and wet conditions, the total porosity of the membrane is calculated according to the formula below:

$$\varepsilon = \frac{m_w - m_d}{\rho_w A l} \quad (2)$$

Where m_w and m_d are dry and wet weights of the membrane respectively (g), A and l are the area (cm^2) and thickness (μm) of membrane respectively, and ρ_w is the density of pure water (g/cm^3).

The Guerout-Elford-Ferry equation was applied to calculate the mean pore diameter of the membrane (Guo et al., 2020):

$$r_m = \sqrt{\frac{(2.9 - 1.75\varepsilon) \times 8\eta l Q}{\varepsilon \times A \times \Delta P}} \quad (3)$$

Where η is the viscosity of water, Q is the penetration rate of pure water(m^3/s), and ΔP is the operation pressure (0.1MPa).

Performance test of ultrafiltration membrane

Static protein adsorption property tests

First, the ultrafiltration membrane of a certain size was immersed in PBS, and ultrasound treatment was performed for 10 minutes. Then, this ultrafiltration membrane was tested for adsorption in BSA-PBS (1.0 g/L). At the end of the adsorption process, according to the Lambert-Beer's law, the concentrations of the BSA-PBS solution before and after the adsorption were measured with a UV-vis spectrophotometer (UV3600, Shimadzu) to obtain the total adsorption amount of BSA on the membrane.

Dynamic separation performance tests

A three-cycle dynamic ultrafiltration experiment was performed in a dead-end filtratiion apparatus to study the separation and antifouling performances of the two kinds of membranes. To obtain stable permeation flux, each membrane was pressurized with deionized water at 0.15 MPa for 30 min. Subsequently, ultrafiltration operation was conducted for 1 h with pure water as the feed solution at a pressure of 0.1 MPa. During this period, the quality of filtrate was recorded every 5 min. The pure water flux (J_w， L/m^{2}h) of the ultrafiltration membrane can be calculated according to the following formula:

$$J = \frac{V}{At} \tag{4}$$

Where A is the effective filtration area (m^2), and V represents the penetration volume （L） of liquid produced by the membrane over the sampling time interval t (h). Subsequently, the BSA-PBS solution was used as the feed solution, and the ultrafiltration process was conducted for 1 h at 0.1 MPa. During this period, the water flux of the protein solution (J_P, L/m^{2}h) was measured every 5 min. Meanwhile, the protein rejection ratio (R) of the ultrafiltration membrane can be calculated by the following formula:

$$R(\%) = \left(1 - \frac{C_p}{C_f}\right) \times 100\% \tag{5}$$

Among them, C_P and C_f represent the concentrations of permeate and feed solutions respectively. To evaluate membrane antifouling property, the concepts of flux recovery ratio (*FRR*), total flux decline ratio (R_t), reversible flux decline ratio (R_r), and irreversible flux decline ratio (R_{ir}) was introduced, which could be calculated by the following equations (Huang et al. 2018):

$$FRR(\%) = \left(\frac{J_{w,i}}{J_{w,i-1}}\right) \times 100 \tag{6}$$

$$R_t(\%) = \left(\frac{J_{w,i-1} - J_{p,i}}{J_{w,i-1}}\right) \times 100 \tag{7}$$

$$R_r(\%) = \left(\frac{J_{w,i} - J_{p,i}}{J_{w,i-1}}\right) \times 100 \tag{8}$$

$$R_{ir}(\%) = \left(\frac{J_{w,i-1} - J_{w,i}}{J_{w,i-1}}\right) \times 100 = R_t - R_r \tag{9}$$

In addition, Darcy's law (Guo et al. 2020) is the basic formula describing fluid flow through porous media, which can be used to explain the relationship between membrane flux and

membrane fouling characteristics. The calculation equations are as follows (Wang et al. 2021):

$$R_t = R_m + R_f = R_m + R_c + R_p = \frac{\Delta P}{\eta \times J_{p,i}} \quad (10)$$

$$R_m = \frac{\Delta P}{\eta \times J_{w,i-1}} \quad (11)$$

$$R_m + R_p = \frac{\Delta P}{\eta \times J_{w,i}} \quad (12)$$

Where R_f, R_t and R_m are the fouling resistance, total hydraulic resistance and membrane resistance, respectively. Where R_f can be divided into R_c and R_p. R_c represents the outer cake layer resistance on the membrane surface, which is related to the reversible fouling; R_p represents the pore blocking resistance in the membrane, which is due to the irreversible fouling.

Results and discussion

Chemical structures of CA and CA-2,3-AD

To have a clear understanding of the chemical structures of the prepared novel materials, FTIR was first used to characterize CA, DAC and CA-2,3-DA. As shown in Fig. 1, two characteristic absorption peaks were found at 1739 cm^{-1} (C=O) and 1221 cm^{-1} (C-O), which should be belonged to the ester group of cellulose acetate (Yu et al. 2019), so these absorption peaks existed in CA, DAC and CA-DA. Besides, as an intermediate product, DAC had an absorption peak belonging to hemiacetal at 775 cm^{-1}(Errokh et al. 2018), indicating that it has been successfully prepared. In the spectra of CA-2,3-DA, two characteristic peaks of the benzene ring appeared at 1517 and 815 cm^{-1} (Guo et al. 2019; Li et al. 2019). This result indicated that dopamine had been successfully modified to CA.

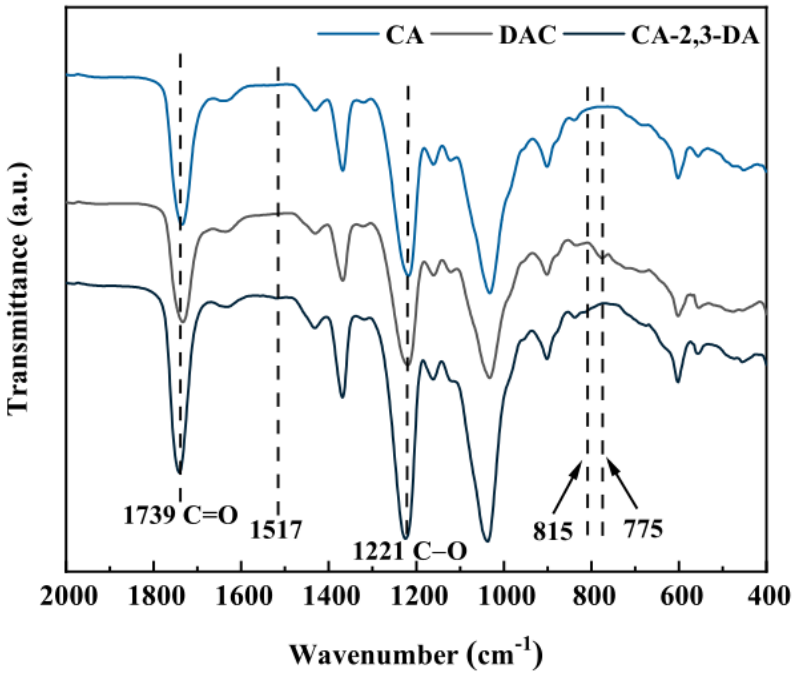

Fig. 1 FTIR spectra of CA, DAC, and CA-2,3-DA

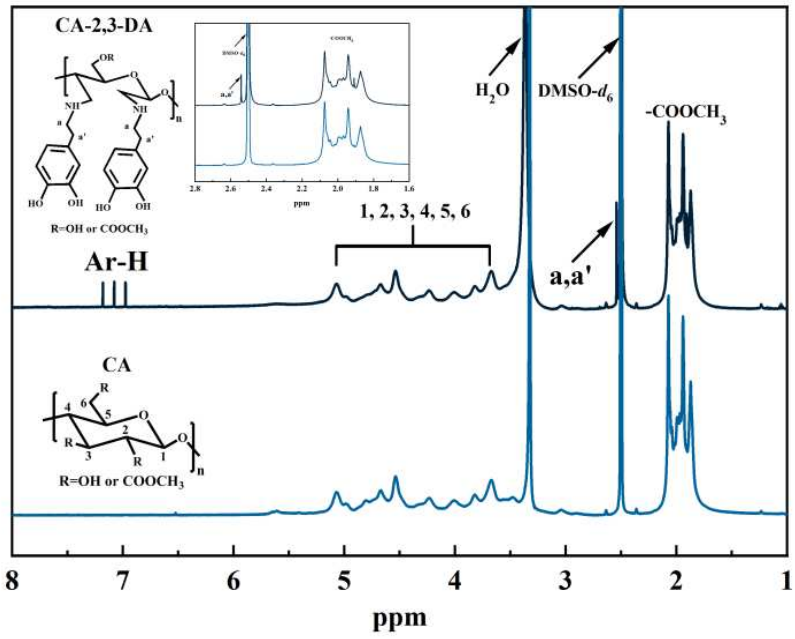

Fig. 2 ^{1}H NMR spectra of CA and CA-2,3-DA.

^{1}H NMR measurement was used to further verify the chemical structure of CA-2,3-DA. As shown in Fig. 2, compared with CA, the spectra of CA-2, 3-DA generated some new peaks at 7.10 and 2.53 ppm, which were the characteristic triplet peaks of the benzene ring and the methylene peak in the dopamine structure, respectively (Khamrai et al. 2019; Zhong et al. 2019). Combined with FTIR and ^{1}H NMR characterizations, it was confirmed that CA was successfully modified by

dopamine.

Fig. 3 showed the TGA curves of CA and CA-2,3-DA. Compared with CA, the thermal decomposition temperature of CA-2,3-DA was significantly lower, which might be the degradation of polymer backbones caused by selective oxidation and decomposition of the side groups. Nevertheless, a decomposition temperature of around 250 ℃ is sufficient to meet the thermal stability requirements of ultrafiltration operation.

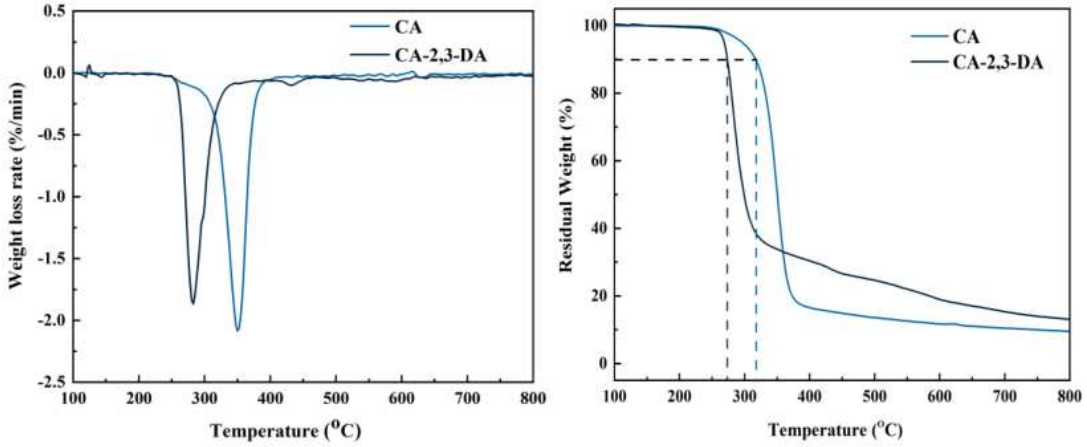

Fig. 3 TGA/DTG curves of CA and CA-2,3-DA.

Characterizations of ultrafiltration membranes

To compare the microstructures of the two types of ultrafiltration membranes, their cross-section and surface morphologies were observed by SEM. (Fig. 4). On the whole, both membranes possess dense surface layers and finger-like pore sublayers, which show the typical characteristics of asymmetric microstructure. Compared with the CA membrane, the CA-2,3-DA membrane had a larger average pore size and porosity (Table 1), and a large number of small pores were formed on the pore wall of the CA-2,3-DA membrane, which were favorable for increasing the permeability. In addition, the CA-2,3-DA membrane had a smoother surface, which could effectively reduce the adhesion and adsorption of pollutants. This result might be attributed to the fact that the introduction of the hydrophilic dopamine accelerated the phase inversion rate during membrane preparation process.

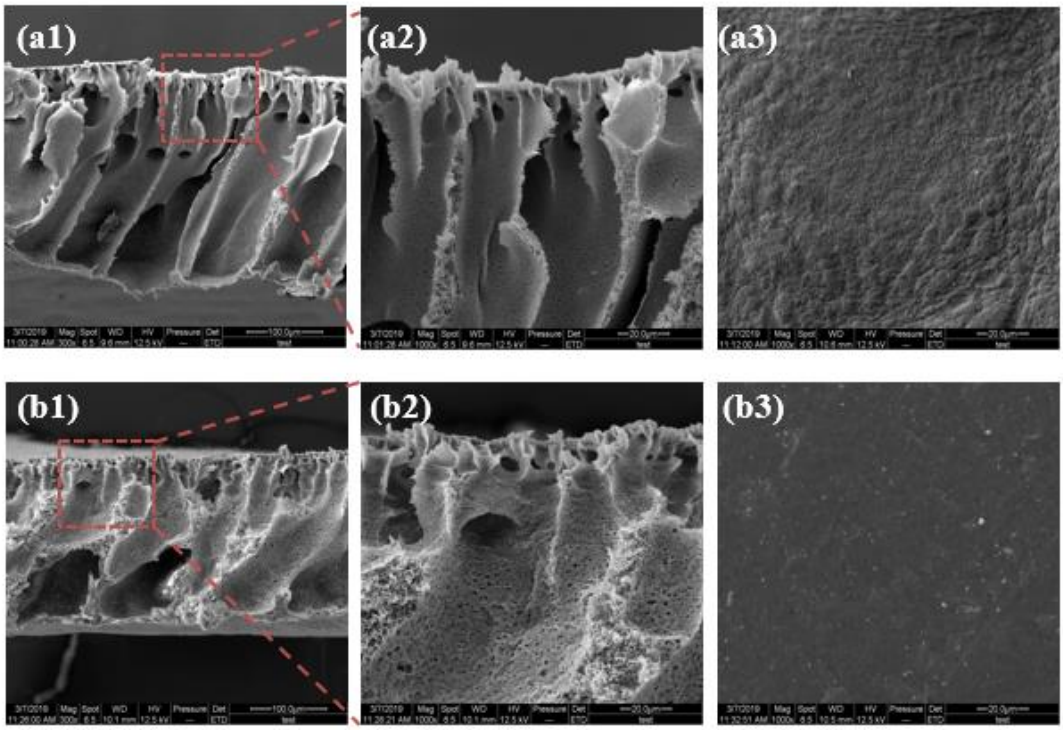

Fig. 4 SEM images of the CA (a) and CA-2,3-DA (b) membranes: (1) the overall cross-section morphology (magnification:300×), (2) the partial cross-section morphology (magnification: 1000×) and (3) the surface morphology (magnification: 1000×).

Table 1 Pore statistics, contact angles and surface energies of the CA and CA-2,3-DA membranes.

membrane	Porosity (%)	Mean pore size (nm)	Contact Angle (°)	Surface energy (mJ/m^2)	BSA adsorption amount ($\mu g/cm^2$)
CA	69.3	21.7	69.8	41.8	41.4
CA-2,3-DA	71.9	28.3	54.1	47.5	21.5

Hydrophilicity is a crucial index to measure the antifouling and permeability performance of membrane materials. WCA is one of the most commonly used and reliable techniques to characterize the hydrophilicity of solid surfaces. Table 1 shows the WCA and surface energies of the CA and CA-2,3-DA membranes. After modification with dopamine, the WCA of CA membrane decreased from 69.8° to 54.1°.

Static protein adsorptions of ultrafiltration membranes

Using BSA as a model contaminant,according to the adsorption amount of protein per unit area on

the membrane surface, the static antifouling performance of the ultrafiltration membrane can be measured. The experimental results are also summarized in Table 1. The protein adsorption capacity of the primordial membrane was 41.4 μg/cm^2, while that of the CA-2,3-DA membrane was significantly decreased to only 21.5 μg/cm^2. Due to the lack of polar interaction between the CA membrane and water molecules, the hydrophobic interaction is the main contributor between the CA membrane and protein molecules, resulting in a mass of BSA adsorbed on the surface of the CA membrane. However, the BSA adsorption on the CA-2,3-DA membrane was less, due to the fact that the introduced dopamine can bind to water molecules and form a hydration layer on the membrane surface, thereby hindering the adsorption of proteins (Khamrai et al. 2019).

Separation performances of ultrafiltration membranes

The separation performance of ultrafiltration membrane is mainly reflected in two aspects, the pure water flux and rejection ratio. Fig.5 illustrates the experimental results of the CA and CA-2,3-DA membranes with distilled water and BSA solution as feed solutions. The water flux of the CA-2,3-DA membrane was 167.3 L/m^{2}h, which was about 2.2 times that of the CA membrane (76.1 L/m^{2}h). One possible explanation for the substantial increase in water flux is that the improved average pore size and of porosity the membrane, the optimized membrane microstructure morphology, and the improved membrane surface hydrophilicity jointly promote the penetration of water molecules. Meanwhile, concerning the BSA rejection ratio, both of them showed excellent performance. Compared with CA membrane, the BSA rejection ratio of CA-2,3-DA membrane increased slightly from 91.9 to 92.5%. In order to evaluate our work, we collected the recently reported the CA-based membranes for comparison, and the comparison results are shown in Fig. 6. In contrast, the CA-2,3-DA membrane exhibited relatively excellent comprehensive separation performance. In general, the CA-2,3-DA membrane maintains a high BSA rejection ratio while having a high water flux, so to some extent we have overcome the long-term challenge of the trade-off relationship between selectivity and permeability in the traditional CA separation membranes.

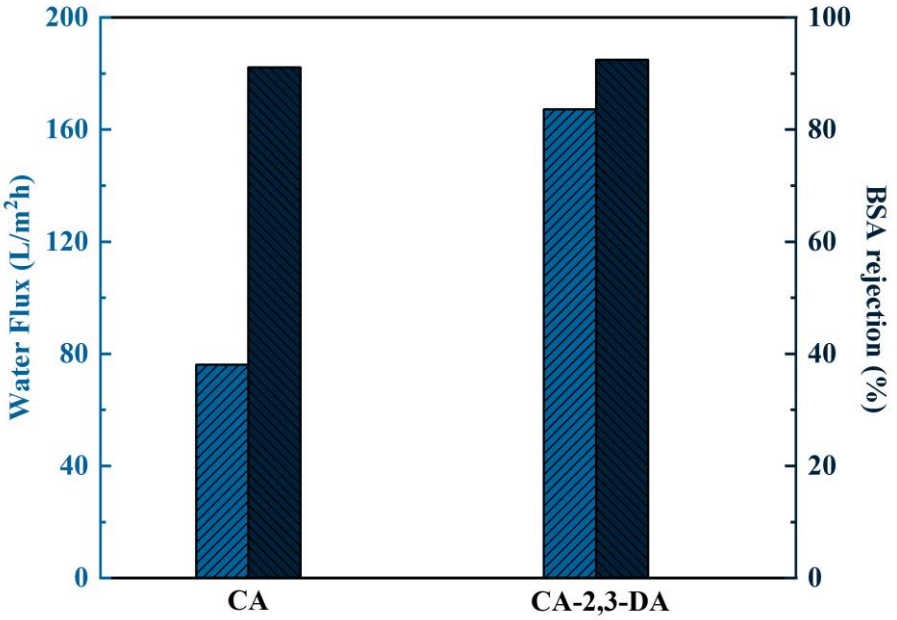

310

311 **Fig. 5** Ultrafiltration performances of the CA and CA-2,3-DA membranes.

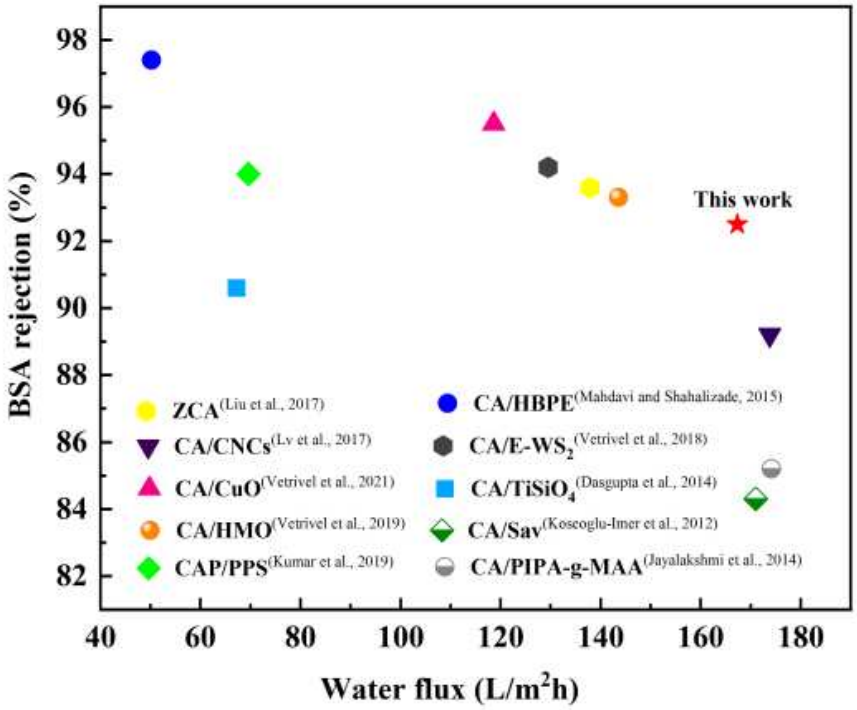

312

313 **Fig. 6** Comparison of BSA rejections and water fluxes for the CA-based membranes reported in

314 the literatures with the CA-2,3-DA membrane used in this work. (Dasgupta et al. 2014;

315 Jayalakshmi et al. 2014; Koseoglu-Imer et al. 2012; Kumar et al. 2019; Liu et al. 2017; Lv et al.

316 2017; Mahdavi and Shahalizade 2015; Vetrivel et al. 2018, 2019, 2021)

317

318

Antifouling properties of ultrafiltration membranes

To evaluate the antifouling performance of the two membranes before and after modification, a three-cycle dynamic ultrafiltration experiment was performed, and the test results are shown in Fig. 7. In the first cycle ends, the flux of both membranes showed a sharp decrease due to membrane fouling. After membrane cleaning, the CA-2,3-DA membrane showed a higher flux recovery ratio (70.9%) than the CA membrane (64.6%), indicating that the CA-2,3-DA membrane had greater potential in antifouling performance. Moreover, to comprehensively monitor membrane fouling, three fouling parameters such as irreversible (R_{ir}), eversible (R_r), and total (R_t) flux decline ratios were calculated and depicted in Fig. 8. It was worth noting that compared with the CA membrane, the CA-2,3-DA membrane significantly increased R_r on the base of lower R_t. This indicated that the fouling layer on the CA-2,3-DA membrane surface was loose and could be removed more easily by physical washing. However, the surface contamination of the CA membrane was controlled by irreversible fouling and could only be mitigated by biological degradation or chemical washing. Consequently, the experimental results showed that the antifouling property of the CA membrane modified by dopamine had been significantly improved, which was advantageous to its application.

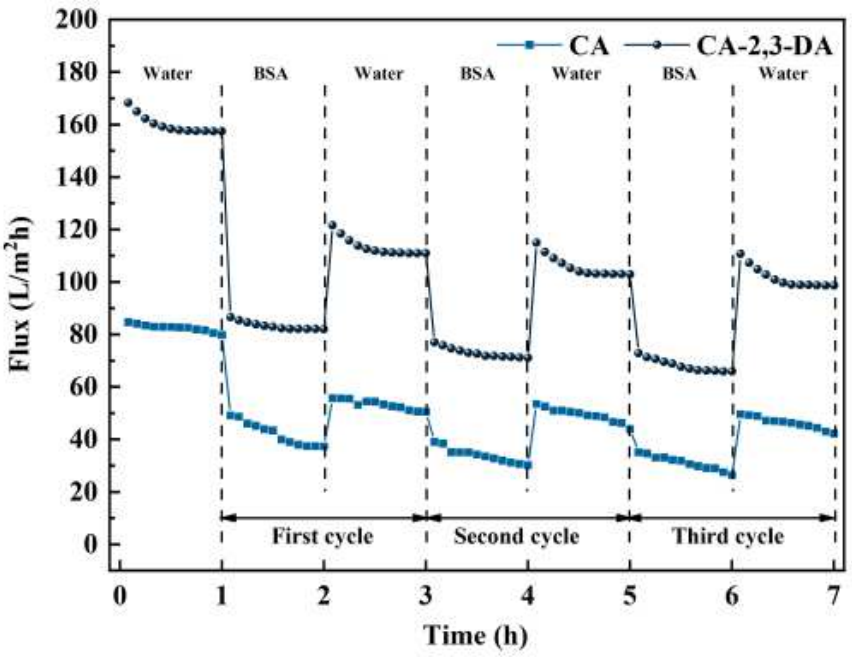

Fig. 7 Time-dependent filtration fluxes of the CA and CA-2,3-DA membranes during three cycles

of the protein ultrafiltration experiment.

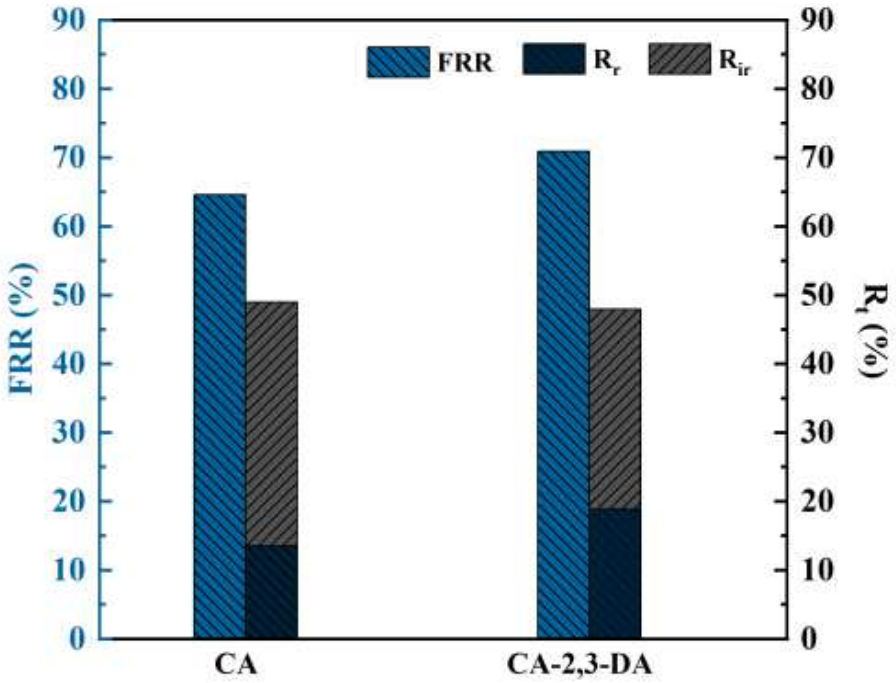

Fig. 8 Summary of the flux recovery ratio (*FRR*), total flux decline ratio ($R_t = R_r + R_{ir}$), reversible flux decline ratio (R_r) and irreversible flux decline ratio (R_{ir}) of the CA and CA-2,3-DA membranes during the protein ultrafiltration experiments.

Through the calculation of filtration resistance, the antifouling performance of the membrane can be more objectively evaluated. As shown in Fig. 9, the R_t of the CA membrane was 2.1 times that of the CA-2,3-DA membrane, which was almost consistent with the relationship between the pure water fluxes of the two membranes mentioned above. The R_m value of the CA membrane was about 1.94 times that of the CA-2,3-DA membrane, which might be related to the intrinsic property, lower average pore size and porosity of the CA membrane. In addition, for R_f value, the CA membrane was 2.02 times of the CA-2,3-DA membrane, indicating that the degree of membrane fouling of the former was much higher than that of the latter. More importantly, for the CA-2,3-DA membranes, the R_c accounted for 55.4% of the R_f, which meant that membrane fouling was dominated by reversible fouling. The results showed that dopamine had a significant effect on improving the antifouling performance of CA membrane.

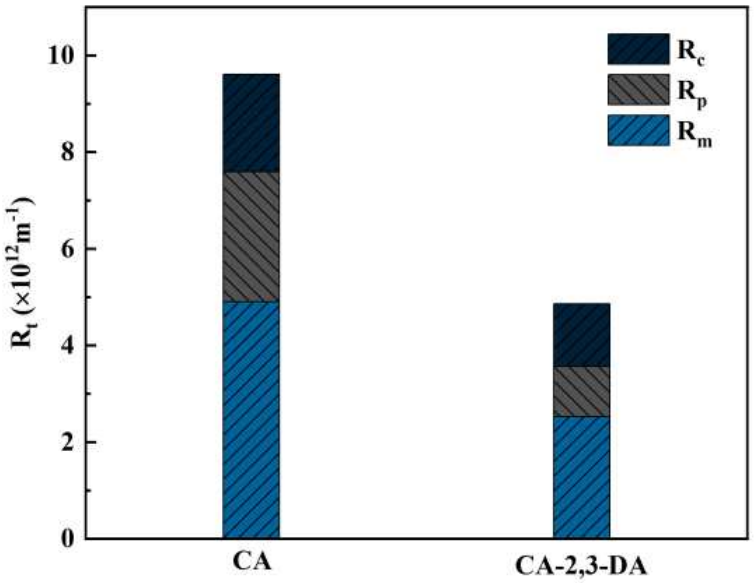

Fig. 9 Summary of the total hydraulic resistance (R_t), membrane resistance (R_m), fouling resistance ($R_f = R_c + R_p$), cake layer resistance (R_c) and pore-blocking resistance (R_p) of the CA and CA-2,3-DA membranes during cycles of the protein ultrafiltration experiment.

Fig.10 shows the FRR of two prepared membranes after different cycles of the protein ultrafiltration experiments. In the first cycle, both membranes showed relatively low *FRR* values, 64.58% for CA membrane and 70.90% for CA-2,3-DA membrane, which were caused by membrane fouling. In the following two cycles, the *FRR* values of both membranes tended to stabilize at a higher level, especially for the CA-2,3-DA membrane was as high as 96.0% in the third cycle. Also, after three cycles of ultrafiltration experiments, the pure water and BSA fluxes of the CA-2,3-DA membrane were as high as 101.6 L/m^{2}h and 68.2 L/m^{2}h, respectively, which were more than 2 times higher than those of the CA membrane. The above experimental results proved that the introduction of dopamine endowed CA membrane with outstanding long-term performance stability and antifouling property, which was beneficial to prolong the service life and cleaning cycle of the membrane.

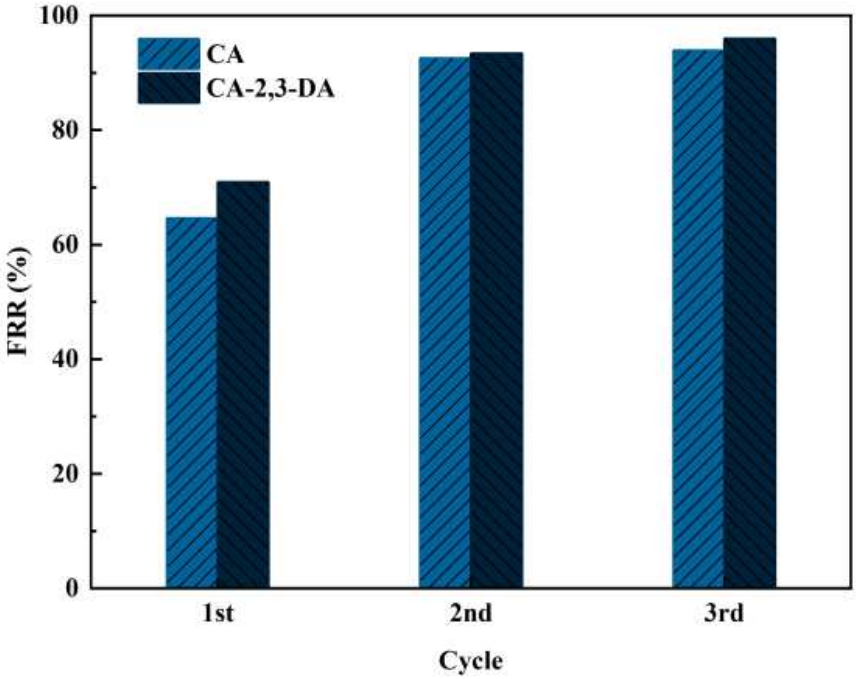

Fig. 10 The flux recovery ratios (*FRR*) of the CA and CA-2,3-DA membranes after various cycles of the protein ultrafiltration experiment.

Conclusions

The application and development of ultrafiltration technology are largely restricted by membrane fouling. Therefore, a scalable method for the production of antifouling membrane by the traditional immersion precipitation phase inversion process was proposed, using a specially designed and prepared dopamine-modified cellulose acetate (CA-2,3-DA) based on selective oxidation and Schiff base reactions as the membrane material. In comparison to the pristine CA membrane, the CA-2,3-DA membrane had much higher permeability with comparable selectivity. In addition, the experimental results of three-cycle dynamic ultrafiltration and static protein adsorption showed that CA-2,3-DA membrane had excellent antifouling performance and high recyclability, which were supported from different angles by parameters such as the filtration resistance, flux recovery ratio and flux decline ratio. In this study, a high-performance membrane material was developed using green and degradable cellulose derivative materials, which greatly expanded the high-value utilization of modified natural organic polysaccharides in separation

388 engineering and its important role in the sustainable development of human society.

389

390 **Acknowledgements** We are thankful for the financial support from the Fundamental Research
391 Funds for the Central Universities (2572021BB07), Natural Science Foundation of Heilongjiang
392 Province (LH2021B003) and Postdoctoral Scientific Research Developmental Fund of
393 Heilongjiang Province (LBH-Q18005), China.

394

395 **References**

396 Chen, X. Y., Deng, E., Park, D., Pfeifer, B. A., Dai, N., Lin, H. Q., 2020. Grafting Activated Graphene
397 Oxide Nanosheets onto Ultrafiltration Membranes Using Polydopamine to Enhance Antifouling
398 Properties. ACS Appl. Mater. Interfaces 12(42), 48179–48187.
399 https://doi.org/10.1021/acsami.0c14210

400 Cheng, D., Liu, Y., Zhang, Y., Ran, J., Bi, S., Deng, Z., Cai, G., Tang, X., Zhou, Y. and Wang, X.,
401 2020. Polydopamine-assisted deposition of CuS nanoparticles on cotton fabrics for photocatalytic
402 and photothermal conversion performance. Cellulose 27(14), 8443-8455.
403 https://doi.org/10.1007/s10570-020-03358-5

404 Choi, Y. S., Kang, H., Kim, D. G., Cha, S. H., Lee, J. C., 2014. Mussel-Inspired Dopamine- and
405 Plant-Based Cardanol-Containing Polymer Coatings for Multifunctional Filtration Membranes.
406 ACS Appl. Mater. Interfaces 6(23), 21297–21307. https://doi.org/10.1021/am506263s

407 Dasgupta, J., Chakraborty, S., Sikder, J., Kumar, R., Pal, D., Curcio, S., Drioli, E., 2014. The effects of
408 thermally stable titanium silicon oxide nanoparticles on structure and performance of cellulose
409 acetate ultrafiltration membranes. Sep. Purif. Technol 133, 55–68.
410 https://doi.org/10.1016/j.seppur.2014.06.035

411 Errokh, A., Magnin, A., Putaux, J. and Boufi, S., 2018. Morphology of the nanocellulose produced by
412 periodate oxidation and reductive treatment of cellulose fibers. Cellulose 25(7), 3899-3911.
413 https://doi.org/10.1007/s10570-018-1871-7

414 Guo, H., Peng, Y., Liu, Y., Wang, Z., Hu, J., Liu, J., Ding, Q., Gu, J., 2020. Development and
415 investigation of novel antifouling cellulose acetate ultrafiltration membrane based on dopamine
416 modification. Int. J. Biol. Macromol 160, 652–659.
417 https://doi.org/10.1016/j.ijbiomac.2020.05.223

418 Guo, H., Wang, Z., Liu, Y., Huo, P., Gu, J., Zhao, F., 2020. Synthesis and characterization of novel
419 zwitterionic poly(aryl ether oxadiazole) ultrafiltration membrane with good antifouling and
420 antibacterial properties. J. Memb. Sci 611, 118337. https://doi.org/10.1016/j.cclet.2007.11.005
421 Guo, T. Y., Gu, L. H., Zhang, Y., Chen, H., Jiang, B., Zhao, H. F., Jin, Y. C., Xiao, H. N., 2019.
422 Bioinspired self-assembled films of carboxymethyl cellulose–dopamine/montmorillonite. J.
423 Mater. Chem. A 7(23), 14033–14041. https://doi.org/10.1039/C9TA00998A
424 Huang, H., Yu, J., Guo, H., Shen, Y., Yang, F., Wang, H., Liu, R., 2018. Improved antifouling
425 performance of ultrafiltration membrane via preparing novel zwitterionic polyimide. Appl. Surf.
426 Sci 427, 38–47. https://doi.org/10.1016/j.apsusc.2017.08.004
427 Jayalakshmi, A., Rajesh, S., Kim, I. C., Senthilkumar, S., Mohan, D., Kwon, Y. N., 2014.
428 Poly(isophthalamide) based graft copolymer for the modification of cellulose acetate
429 ultrafiltration membranes and a fouling study by AFM imaging. J. Memb. Sci 465, 117–128.
430 https://doi.org/10.1016/j.memsci.2014.04.020
431 Kallem, P., Ibrahim, Y., Hasan, S. W., Show, P. L., Banat, F., 2021. Fabrication of novel
432 polyethersulfone (PES) hybrid ultrafiltration membranes with superior permeability and
433 antifouling properties using environmentally friendly sulfonated functionalized polydopamine
434 nanofillers. Sep. Purif. Technol 261, 118311. https://doi.org/10.1016/j.seppur.2021.118311
435 Karami, P., Khorshidi, B., McGregor, M., Peichel, J. T., Soares, J. B. P., Sadrzadeh, M., 2020.
436 Thermally stable thin film composite polymeric membranes for water treatment: A review. J.
437 Clean. Prod 250, 119447. https://doi.org/10.1016/j.jclepro.2019.119447
438 Keating, J. J., Imbrogno, J., Belfort, G., 2016. Polymer Brushes for Membrane Separations: A Review.
439 ACS Appl. Mater. Interfaces 8(42), 28383–28399. https://doi.org/10.1021/acsami.6b09068
440 Khamrai, M., Banerjee, S. L., Paul, S., Ghosh, A. K., Sarkar, P., Kundu, P. P., 2019. A Mussel Mimetic,
441 Bioadhesive, Antimicrobial Patch Based on Dopamine-Modified Bacterial Cellulose/rGO/Ag
442 NPs: A Green Approach toward Wound-Healing Applications. ACS Sustain. Chem. Eng 51(4),
443 12083-12097. https://doi.org/10.1021/acssuschemeng.9b01163
444 Koseoglu-Imer, D. Y., Dizge, N., Koyuncu, I., 2012. Enzymatic activation of cellulose acetate
445 membrane for reducing of protein fouling. Colloids Surfaces B Biointerfaces 92, 334–339.
446 https://doi.org/10.1016/j.colsurfb.2011.12.013
447 Kumar, M., RaoT., S., Isloor, A. M., Ibrahim, G. P. S., Inamuddin, Ismail, N., Ismail, A. F., Asiri, A.

M., 2019. Use of cellulose acetate/polyphenylsulfone derivatives to fabricate ultrafiltration hollow fiber membranes for the removal of arsenic from drinking water. Int. J. Biol. Macromol 129, 715–727. https://doi.org/10.1016/j.ijbiomac.2019.02.017

Li, M., Wu, Z., Luo, M., Wang, W., Chang, K., Liu, K., Liu, Q., Xia, M. and Wang, D., 2015. Highly hydrophilic and anti-fouling cellulose thin film composite membrane based on the hierarchical poly(vinyl alcohol-co-ethylene) nanofiber substrate. Cellulose 22(4), 2717-2727. https://doi.org/10.1007/s10570-015-0682-3

Li, K., Jin, S. C., Chen, H., Li, J. Z., 2019. Bioinspired interface engineering of gelatin/cellulose nanofibrils nanocomposites with high mechanical performance and antibacterial properties for active packaging. Compos. Part B Eng 171, 222–234. https://doi.org/10.1016/j.compositesb.2019.04.043

Li, R. J., Li, J. Y., Rao, L. H., Lin, H. J., Shen, L. G., Xu, Y. C., Chen, J. R., Liao, B. Q., 2021. Inkjet printing of dopamine followed by UV light irradiation to modify mussel-inspired PVDF membrane for efficient oil-water separation. J. Memb. Sci 619, 118790. https://doi.org/10.1016/j.memsci.2020.118790

Liu, C. H., Lee, J. H., Ma, J., Elimelech, M., 2017. Antifouling Thin-Film Composite Membranes by Controlled Architecture of Zwitterionic Polymer Brush Layer. Environ. Sci. Technol 51(4), 2161–2169. https://doi.org/10.1021/acs.est.6b05992

Liu, S. X., Kim, J. T., 2011. Characterization of Surface Modification of Polyethersulfone Membrane. J. Adhes. Sci. Technol 25(1–3), 193–212. https://doi.org/10.1163/016942410X503311

Liu, Y., Huang, H., Huo, P., Gu, J., 2017. Exploration of zwitterionic cellulose acetate antifouling ultrafiltration membrane for bovine serum albumin (BSA) separation. Carbohydr. Polym 165, 266–275. https://doi.org/10.1016/j.carbpol.2017.02.052

Lv, J. L., Zhang, G. Q., Zhang, H. M., Yang, F. L., 2017. Exploration of permeability and antifouling performance on modified cellulose acetate ultrafiltration membrane with cellulose nanocrystals. Carbohydr. Polym 174, 190–199. https://doi.org/10.1016/j.carbpol.2017.06.064

Mahdavi, H., Shahalizade, T., 2015. Preparation, characterization and performance study of cellulose acetate membranes modified by aliphatic hyperbranched polyester. J. Memb. Sci 473, 256–266. https://doi.org/10.1016/j.memsci.2014.09.013

Mokhena, T., Jacobs, N. and Luyt, A., 2017. Nanofibrous alginate membrane coated with cellulose

478 nanowhiskers for water purification. Cellulose 25(1), 417-427.
479 https://doi.org/10.1007/s10570-017-1541-1
480 Mu, Y. F., Feng, H., Zhang, S. L., Zhang, C. Y., Lu, N., Luan, J. S., Wang, G. Bin., 2020.
481 Development of highly permeable and antifouling ultrafiltration membranes based on the
482 synergistic effect of carboxylated polysulfone and bio-inspired co-deposition modified
483 hydroxyapatite nanotubes. J. Colloid Interface Sci 572, 48–61.
484 https://doi.org/10.1016/j.jcis.2020.03.072
485 Oprea, M., Voicu, S. I., 2020. Recent Advances in Applications of Cellulose Derivatives-Based
486 Composite Membranes with Hydroxyapatite. Materials (Basel) 13(11), 2481.
487 https://doi.org/10.3390/ma13112481
488 Park, H. B., Kamcev, J., Robeson, L. M., Elimelech, M., Freeman, B. D., 2017. Maximizing the right
489 stuff: The trade-off between membrane permeability and selectivity. Science 356(6343),
490 eaab0530. https://doi.org/10.1126/science.aab0530
491 Rafieian, F., Mousavi, M., Dufresne, A., Yu, Q., 2020. Polyethersulfone membrane embedded with
492 amine functionalized microcrystalline cellulose. Int. J. Biol. Macromol 164, 4444–4454.
493 https://doi.org/10.1016/j.ijbiomac.2020.09.017
494 Silva, M. A., Belmonte-Reche, E., de Amorim, M. T. P., 2021. Morphology and water flux of produced
495 cellulose acetate membranes reinforced by the design of experiments (DOE). Carbohydr. Polym
496 254, 117407. https://doi.org/10.1016/j.carbpol.2020.117407
497 Tian, H. L., Wu, X., Zhang, K. S., 2021. Polydopamine-Assisted Two-Dimensional Molybdenum
498 Disulfide (MoS2)-Modified PES Tight Ultrafiltration Mixed-Matrix Membranes: Enhanced Dye
499 Separation Performance. Membranes 11(2), 96. https://doi.org/10.3390/membranes11020096
500 Vetrivel, S., Rana, D., Sri Abirami Saraswathi, M. S., Divya, K., Kaleekkal, N. J., Nagendran, A., 2019.
501 Cellulose acetate nanocomposite ultrafiltration membranes tailored with hydrous manganese
502 dioxide nanoparticles for water treatment applications. Polym. Adv. Technol 30(8), 1943–1950.
503 https://doi.org/10.1002/pat.4626
504 Vetrivel, S., Saraswathi, M. S. S. A., Rana, D., Divya, K., Nagendran, A., 2021. Cellulose acetate
505 ultrafiltration membranes customized with copper oxide nanoparticles for efficient separation
506 with antifouling behavior. J. Appl. Polym. Sci 138(8), 49867. https://doi.org/10.1002/app.49867
507 Vetrivel, S., Sri Abirami Saraswathi, M., Rana, D., Divya, K., Nagendran, A., 2018. Cellulose acetate

composite membranes tailored with exfoliated tungsten disulfide nanosheets: Permeation characteristics and antifouling ability. Int. J. Biol. Macromol 115, 540–546. https://doi.org/10.1016/j.ijbiomac.2018.04.091

Wang, J. L., Liu, X. J. (2021). Forward osmosis technology for water treatment: Recent advances and future perspectives. J. Clean. Prod 280, 124354. https://doi.org/10.1016/j.jclepro.2020.124354

Wang, M., Xu, Z. W., Guo, Y. L., Hou, Y. F., Li, P., Niu, Q. J., 2020. Engineering a superwettable polyolefin membrane for highly efficient oil/water separation with excellent self-cleaning and photo-catalysis degradation property. J. Memb. Sci 611, 118409. https://doi.org/10.1016/j.memsci.2020.118409

Wang, Z., Chen, P., Liu, Y., Guo, H., Sun, N., Cai, Q., Yu, Y., Zhao, F., 2021. Exploration of antifouling zwitterionic polyimide ultrafiltration membrane based on novel aromatic diamine monomer. Sep. Purif. Technol 255, 117738. https://doi.org/10.1016/j.seppur.2020.117738

Xie, W. C., Li, T., Tiraferri, A., Drioli, E., Figoli, A., Crittenden, J. C., Liu, B. C., 2021. Toward the Next Generation of Sustainable Membranes from Green Chemistry Principles. ACS Sustain. Chem. Eng 9(1), 50–75. https://doi.org/10.1021/acssuschemeng.0c07119

Yang, J., Zhang, Z. Z., Xu, X. H., Zhu, X. T., Men, X. H., Zhou, X. Y., 2012. Superhydrophilic–superoleophobic coatings. J. Mater. Chem 22(7), 2834. https://doi.org/10.1039/c2jm15987b

Yu, D. Y., Wang, Y. J., Wu, M. H., Zhang, L., Wang, L. L., Ni, H. G., 2019. Surface functionalization of cellulose with hyperbranched polyamide for efficient adsorption of organic dyes and heavy metals. J. Clean. Prod 232, 774–783. https://doi.org/10.1016/j.jclepro.2019.06.024

Yu, S., Kang, G. D., Zhu, Z. H., Zhou, M. Q., Yu, H. J., Cao, Y. M., 2021. Nafion-PTFE hollow fiber composite membranes for improvement of anti-fouling and anti-wetting properties in vacuum membrane distillation. J. Memb. Sci 620, 118915. https://doi.org/10.1016/j.memsci.2020.118915

Zhang, J. S., Loong, W. L. C., Chou, S. R., Tang, C. Y., Wang, R., Fane, A. G., 2012. Membrane biofouling and scaling in forward osmosis membrane bioreactor. J. Memb. Sci 403, 8–14. https://doi.org/10.1016/j.memsci.2012.01.032

Zhong, Y. J., Wang, J., Yuan, Z. Y., Wang, Y., Xi, Z. H., Li, L., Liu, Z. Y., Guo, X. H., 2019. A mussel-inspired carboxymethyl cellulose hydrogel with enhanced adhesiveness through enzymatic crosslinking. Colloids Surfaces B Biointerfaces 179, 462–469.

https://doi.org/10.1016/j.colsurfb.2019.03.044

Zhou, L., Ke, K., Yang, M. B., Yang, W., 2021. Recent progress on chemical modification of cellulose for high mechanical-performance Poly(lactic acid)/Cellulose composite: A review. Compos. Commun 23, 100548. https://doi.org/10.1016/j.coco.2020.100548

Zhu, L. J., Liu, F., Yu, X. M., Xue, L. X., 2015. Poly(Lactic Acid) Hemodialysis Membranes with Poly(Lactic Acid)- block -Poly(2-Hydroxyethyl Methacrylate) Copolymer As Additive: Preparation, Characterization, and Performance. ACS Appl. Mater. Interfaces 7(32), 17748–17755. https://doi.org/10.1021/acsami.5b03951

Declaration of interests

The authors declare that they have no known competing financial interests or personal relationships that could have appeared to influence the work reported in this paper.

Supplementary Files

This is a list of supplementary files associated with this preprint. Click to download.

- GraphicalAbstract.jpg